Brovchenko, I., Maderich, V., Terletska, K., & Bezhenar, A. (2020)
Modelling seasonal and intraseasonal variations of circulation,
temperature, salinity and sea level in the Bellingshausen Sea
and on the Antarctic Peninsula shelf.
Ukrainian Antarctic Journal, 2, 16—25.
https://doi.org/10.33275/1727-7485.2.2020.649

I. Brovchenko, V. Maderich*, K. Terletska, A. Bezhenar
Institute of Mathematical Machine and System Problems of NAS of Ukraine, Kyiv, 03187, Ukraine
*** Corresponding author:** vladmad@gmail.com

Modelling seasonal and intraseasonal variations of circulation, temperature, salinity and sea level in the Bellingshausen Sea and on the Antarctic Peninsula shelf

Abstract. The objective of the study is to simulate using numerical methods the seasonal and intraseasonal variations of circulation, sea level, temperature and salinity in the Bellingshausen Sea and on the shelf of the western part of the Antarctic Peninsula (WAP). The Semi-implicit Cross-scale Hydroscience Integrated System Model with an unstructured triangular horizontal grid and a vertical local sigma coordinate system and ice dynamic-thermodynamic Finite-Element Sea Ice Model were applied. Heat, momentum and salt fluxes were set on the ocean surface using the ERA5 reanalysis data. At the open boundaries, the vertical distribution of temperature and salinity was determined according to the COPERNICUS reanalysis. At the western open boundary of the computational domain, the vertical distribution of velocity of currents from COPERNICUS was also specified, whereas at the open eastern boundary the level deviations were specified. Time variability analysis of sea level was performed using wavelet analysis. The results of modelling of the sea level, temperature, and salinity fields for 2014–2015 were compared with the available observational data on the shelf of the WAP, including data from the Ukrainian Antarctic Expedition. The simulated horizontal and vertical distributions of the subsurface layer with minimum of potential temperature T_{min} (Winter Water) are given. The depth of the T_{min} varies in the range of 10–100 m increasing to the north. The values of minimum of potential temperature T_{min} also increase to the north from −1.8 to 1.2 °C. The intraseasonal oscillations of sea level computed by the model for 2014—2015 were analysed together with data of observations at the tidal stations Faraday/Akademik Vernadsky and Rothera located at the coast of WAP. In the range 1–150 days the largest amplitudes of the level scalegrams were found for a period of approximately 100 days in 2014 and 120 days in 2015 at both stations. The largest amplitudes of modelled level scalegrams were observed with a period of approximately 88 days in 2014 and 80 days in 2015 at both stations. The largest amplitudes of scalegrams for Antarctic Oscillation (AAO) were found for a period of 105 days in 2014 and 123 days in 2015. The corresponding correlation coefficients between observed sea level scalegrams and AAO for 2014 were 0.84 and 0.86, respectively, whereas for 2015 they were 0.87 and 0.90, respectively. It was concluded that the relationship between intraseasonal processes in the ocean in West Antarctica and AAO existed at a time scale of about 100 days.

Keywords: Antarctic Peninsula, Bellingshausen Sea, Faraday/Akademik Vernadsky Station, intra-seasonal variations, SCHISM model, Winter Water

1 Introduction

Several important factors control ice and ocean processes in the Bellingshausen Sea. There is a continental shelf along 1200 km of the western part of the Antarctic Peninsula (WAP), which has a width of about 200 km and an average depth of ~450 m. This shelf is in many places intersected by deep canyons reaching depths of 1500 m. The Antarctic Peninsula deflects the Antarctic Circumpolar Current (ACC) north-

ward, so that the Southern Front of the ACC is at a distance of 100–200 km from the shelf (Smith et al., 1999). Unlike other parts of Antarctica, the WAP area does not have a front at the shelf boundary that separates ACC water from shelf water. Therefore, under the upper layer of winter and summer Antarctic Surface Water, on the shelf there is a deep water mass of Circumpolar Deep Water (CDW), which is warmer and saltier than surface water. Often CDW has the nature of intrusions that extend deeply into the shelf due to the canyon topography (Klinck et al., 2004). Another important mechanism of horizontal transfer and mixing on the shelf are shelf-scale cyclonic vortices. Small-scale vortices with internal Rossby radius of 3–5 km can also affect heat transport at the shelf (Graham et al., 2016). Significant seasonal changes are observed in the Bellingshausen Sea primarily due to the formation of ice cover in winter and seasonal wind variations. Winter convection mixes water at the depth of 5–150 m which is capped by warmed-in-summer water, forming subsurface temperature minimum known as Winter Water (WW) (Gordon, 1971; Klinck et al., 2004; Martinson et al., 2008; Moffat & Meredith, 2018). This layer was also observed at the shelf (Neverovsky et al., 2015). A number of models were applied to describe WAP shelf circulation (e.g. Holland et al., 2010; Dinniman et al., 2011; Graham et al., 2016; Regan et al., 2018). All of them used structured grid. However, results of the modelling show necessity of combined use of high resolution (Graham et al., 2016), regional coverage and long-term integration. Therefore, use of unstructured grid models, which allows specifying high resolution at shelf and coarser resolution in the open ocean, has good potential for WAP (Maderich et al., 2018). In the paper, the Semi-implicit Cross-scale Hydroscience Integrated System Model (SCHISM) (Zhang et al., 2016) augmented by Finite-Element Sea Ice Model (FESIM) (Danilov et al., 2015) was used to simulate seasonal and intraseasonal variations of circulation, sea level and thermohaline structure.

2 Methods and data

Modelling of circulation in the Bellingshausen Sea was performed using the unstructured SCHISM model (Zhang et al., 2015; 2016). The equations of the model are the Reynolds-averaged Navier-Stokes equations in the hydrostatic and Boussinesq approximations, which allow calculating the three components of the velocity vector, potential temperature, salinity, and free surface deviation. Kinematic conditions for the free surface are used on the ocean surface. Wind stresses, turbulent heat and moisture fluxes are calculated using a model for the surface layer of the atmosphere (Zeng et al., 1998). At the bottom, the non-slip and the no-flux of heat and salt conditions were used.

The sea ice model in the SCHISM model was adapted from the FESIM model (Danilov et al., 2015). The equations of this model consist of the equations of motion of ice, the transport equations of ice thickness, snow cover thickness and ice concentration. Well-known difficulties in solving the ice dynamics equation are caused by the term of the internal stress, which makes the equations hard to solve and imposes constraints on the time step. The SCHISM model used the addition of pseudo-elasticity, which leads to the elastic-viscous-plastic (EVP) approach (Hunke & Dukowicz, 1997) improved by Bouillon et al. (2013).

SCHISM uses a mixed triangular-quadrangular unstructured horizontal grid and the new vertical coordinate system LSC^2 (Localized Sigma Coordinates). It minimizes the slope of the coordinate planes and at the same time describes the bottom without the appearance of steps, as for the so-called z-coordinate systems, and also has a smooth transition between computing cells, both vertically and horizontally. Other important differences are the use of an implicit advection scheme for second-order transport (TVD^2), an impulse advection scheme and a horizontal viscosity scheme (including biharmonic viscosity) for the efficient inertial spurious filtering without the introduction of excessive dissipation.

Daily data of calculations of currents, sea level, temperature and salinity were performed for the period of 2014–2015. The calculation domain (90–55° W and 53–73° S) includes the WAP shelf, the Bellingshausen Sea and the adjacent part of the Southern Ocean (Fig. 1a). The calculation grid was built using the General Bathymetric Chart of the Oceans database (GEBCO, 2020). The triangular unstructured grid consists of 89,000 elements (Fig. 1a) with a finest

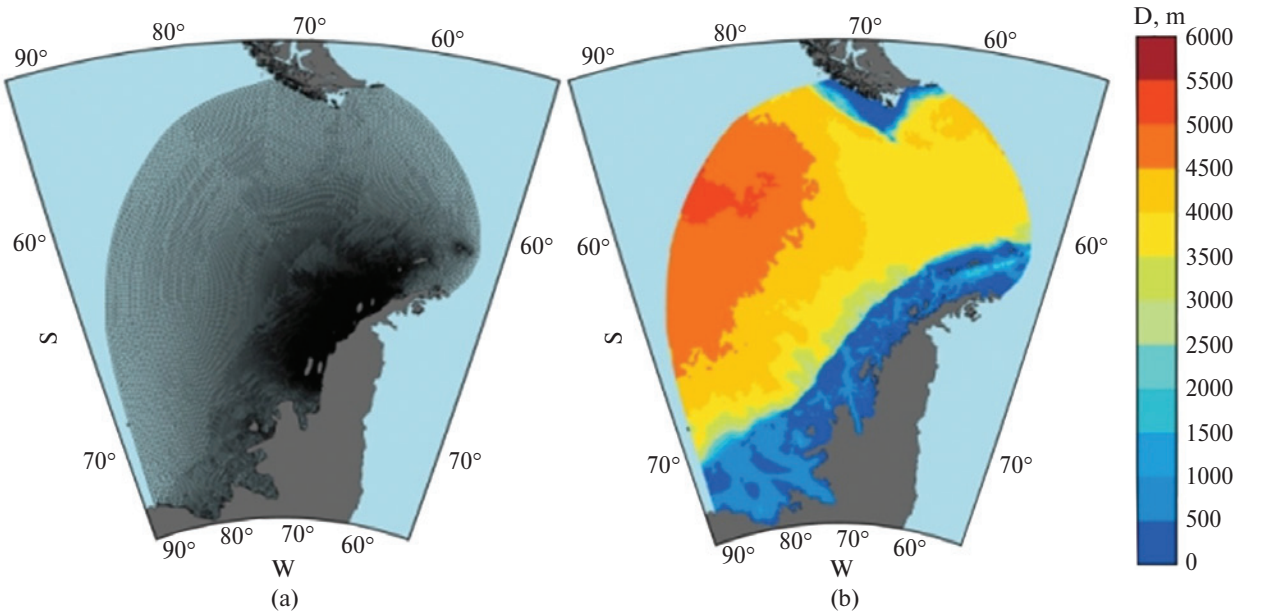

Figure 1. Computational grid (a); distribution of depths in the computational domain in the Bellingshausen Sea according to (GEBCO, 2020) (b)

resolution of 2 km on the WAP shelf (Fig. 1b). The areas in the south of the Bellingshausen Sea occupied by shelf glaciers were not included in the calculations. Vertically, 49 main layers were used.

The air temperature, wind speed, pressure, dew point, cloudiness, precipitation, shortwave and longwave radiations from the reanalysis of meteorological parameters ERA5 (2020) were used. These data were interpolated for the calculation area and were updated every hour. There were no heat and salt fluxes and no-slip conditions for velocities at the solid lateral boundaries. At the western open boundary, the vertical distribution of temperature, salinity and velocity was set according to the COPERNICUS ocean global reanalysis (COPERNICUS, 2020). At the eastern boundary of the calculation area, the vertical distribution of temperature, salinity and elevation from COPERNICUS were set. Ice thickness and concentration at the boundary were nudged from COPERNICUS (2020) data. The distribution of potential temperature and salinity from ocean global reanalysis (COPERNICUS, 2020) were used as initial conditions. The kinetic energy was monitored from the beginning of the calculations, which showed that the model spin-up took several weeks.

The time series analysis $f_k = f(t_k)$, $k = \overline{1, N}$ was carried out by using the wavelet method (Scargle,1997; Torrence & Compo, 1998). Wavelet spectrum estimates, or scalegrams, were calculated by averaging on shifts of the scalograms $S(a_i, b_k)$ (Scargle, 1997).

$$SC(a_i) = \frac{1}{N}\sum_{k=1}^{N} S(a_i, b_k). \quad (1)$$

Scale and shift of energy distribution were described by a scalogram

$$S(a_i, b_i) = \left|W_A(a_i, b_i)\right|^2. \quad (2)$$

The wavelet coefficients $W_A(a_i, b_j)$ are calculated using the MATLAB (2020) software package with Morlet function

$$\psi(\tau) = \exp(-\tau^2/2)\cos(5\tau), \quad (3)$$

where τ is nondimensional time parameter (MATLAB, 2020). The parameter a_i is the scale of wavelet. The parameter b_j is the shift of the wavelet localizing wavelet in time.

3 Results

A common feature of Antarctic water masses is a seasonal formation of the subsurface layer with mini-

ISSN 1727-7485. Ukrainian Antarctic Journal, 2, 2020, https://doi.org/10.33275/1727-7485.2.2020.649

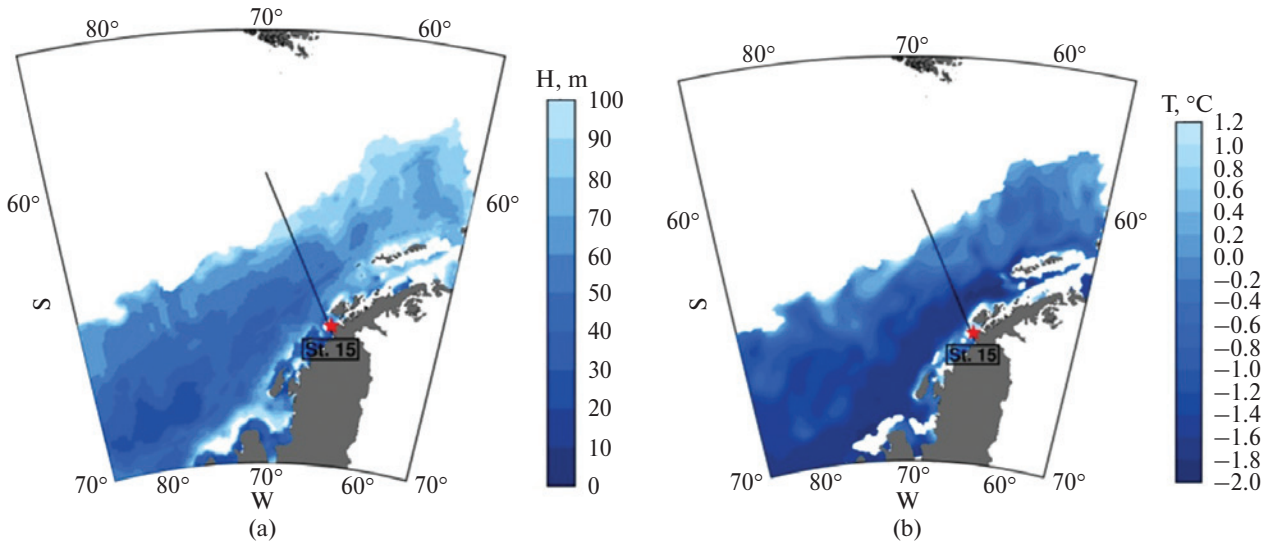

Figure 2. Distribution of the depth H of minimum of potential temperature T_{min} in the Bellinghausen Sea (a) and distribution of T_{min} at the depth H of the minimum of potential temperature (b) for January 2014. The position of the vertical section of T (Fig. 3) is shown by the black line. The star shows location of Station 15 (Fig. 4)

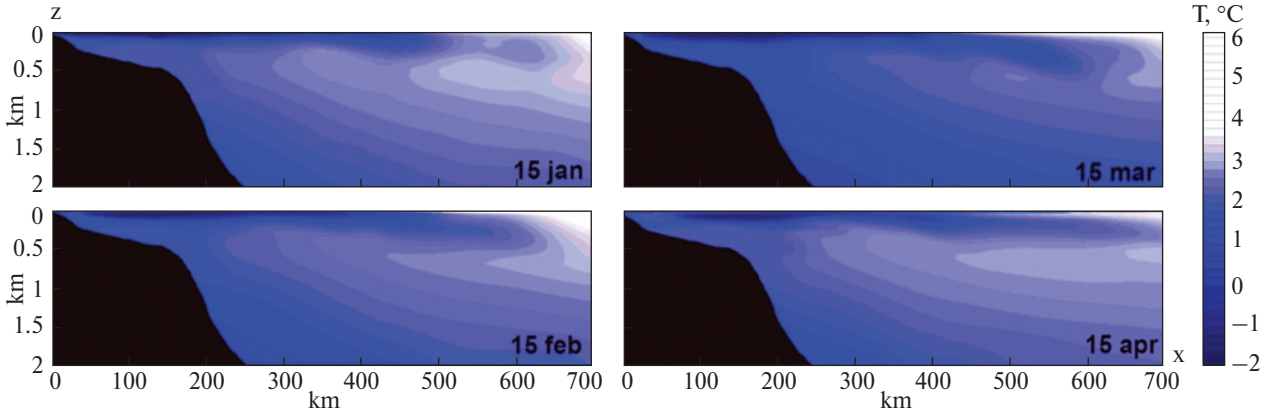

Figure 3. Vertical section of potential temperature T calculated for 15 January, 15 February, 15 March and 15 April 2014 along the cross section shown in Fig. 2

mum of potential temperature T_{min} (Winter Water), which is a remnant of mixed layer formed as a result of convection in the austral winter. The calculated distribution of the depth of T_{min} in the Bellingshausen Sea and distribution of T_{min} at the depth H of the minimum of potential temperature for January 2014 are shown in Fig. 2. The T_{min} depth H varies in the range 10–100 m increasing to the north. The value of T_{min} also increases to the north from –1.8 °C to 1.2 °C. The structure of WW is shown in Fig. 3 where the vertical section of potential temperature T (black line in Fig. 2) is given. Here x is a distance from coast and z is a depth. The temperature in the WW layer slowly decays during austral summer and autumn.

The calculated vertical profiles of the temperature and salinity at WAP shelf are compared in Fig. 4 with the vertical distribution of temperature and salinity at observation Station 15 (65°14.954′ S, 64°13.028′ W) located on the Argentine Islands shelf (Fig. 2). The calculated vertical temperature distributions agreed

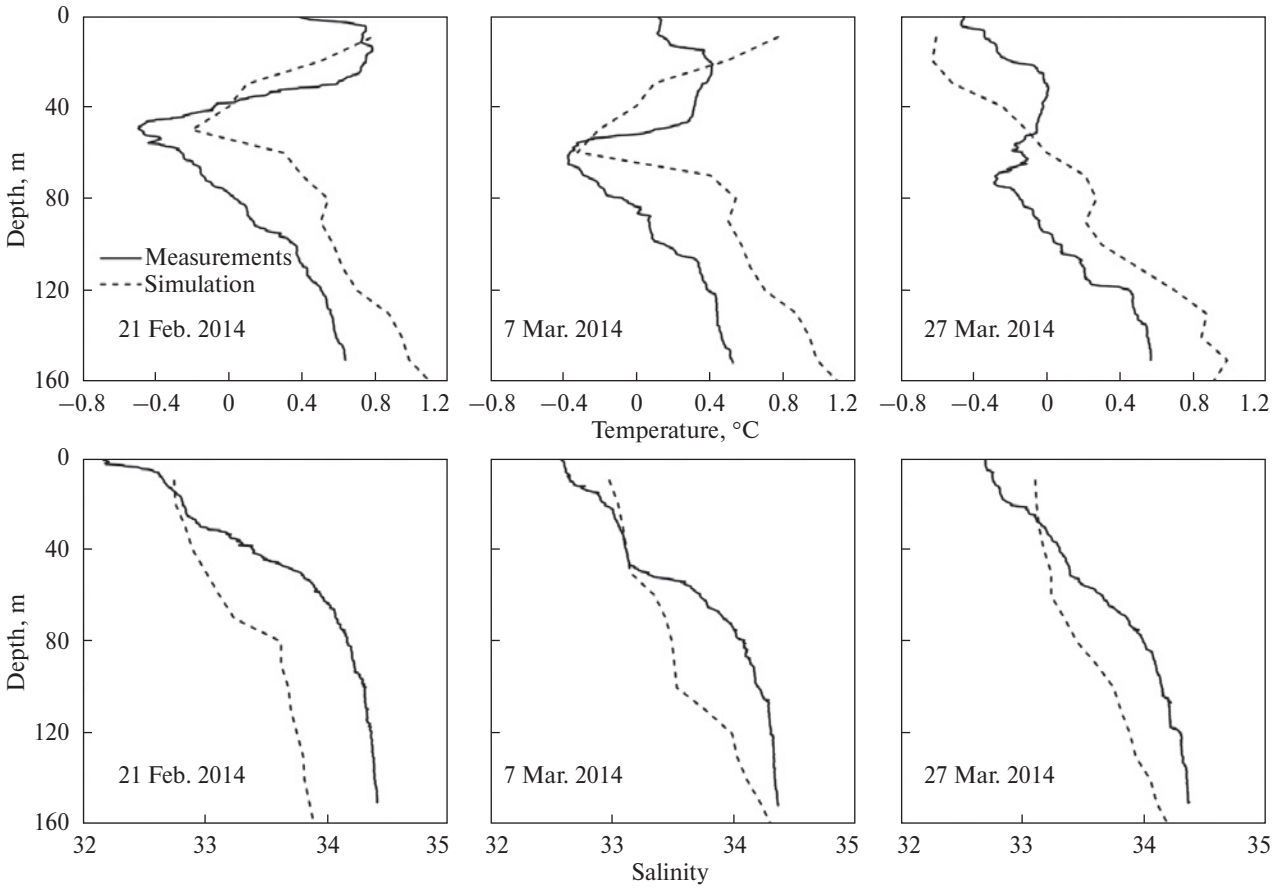

Figure 4. Comparison of calculations (dashed line) and measurements (solid line) of vertical distribution of temperature (a) and salinity (b) on Station 15 (65°14.954′ S, 64°13.028′ W)

with the observations, in particular with the positions and the values of minimum temperature T_{min} on the shelf around the Argentine Islands.

The climate of the Antarctica, and, in particular, the Bellingshausen Sea, is characterized by wide range of oscillations. The interannual variability of sea level at station Faraday/Akademik Vernadsky was studied by Maderich et al. (2019). The wavelet analysis showed presence of maximums in the scalegrams of marine and atmospheric parameters on WAP for the periods of 3–4 years and 6–8 years that confirms the relationship between processes in the atmosphere and ocean in West Antarctica with the natural fluctuations of the ocean-atmosphere system, such as Southern Annular Mode (SAM) or Antarctic Oscillation (AAO) and El Niño Southern Oscillation (ENSO), which have typical periods of 3–4 and 6–8 years. Here the intraseasonal oscillations of sea level computed by the model for 2014–2015 are analysed together with data of observations in tidal stations Faraday/Akademik Vernadsky and Rothera located at the coast of WAP.

The observed daily sea levels at the Faraday/Akademik Vernadsky and Rothera stations (UHSLC, 2020) deviated from the mean value for 2014–2015. The corresponding deviations of sea level (elevations) calculated by the model were imposed on the observed elevations in Fig. 5. As seen in the figure, despite the differences between simulated and observed values, which can be explained by insufficient resolution of the coastal bathymetry by the model and insufficient spatial resolution of wind reanalysis, the simulation and observation are in general agreement.

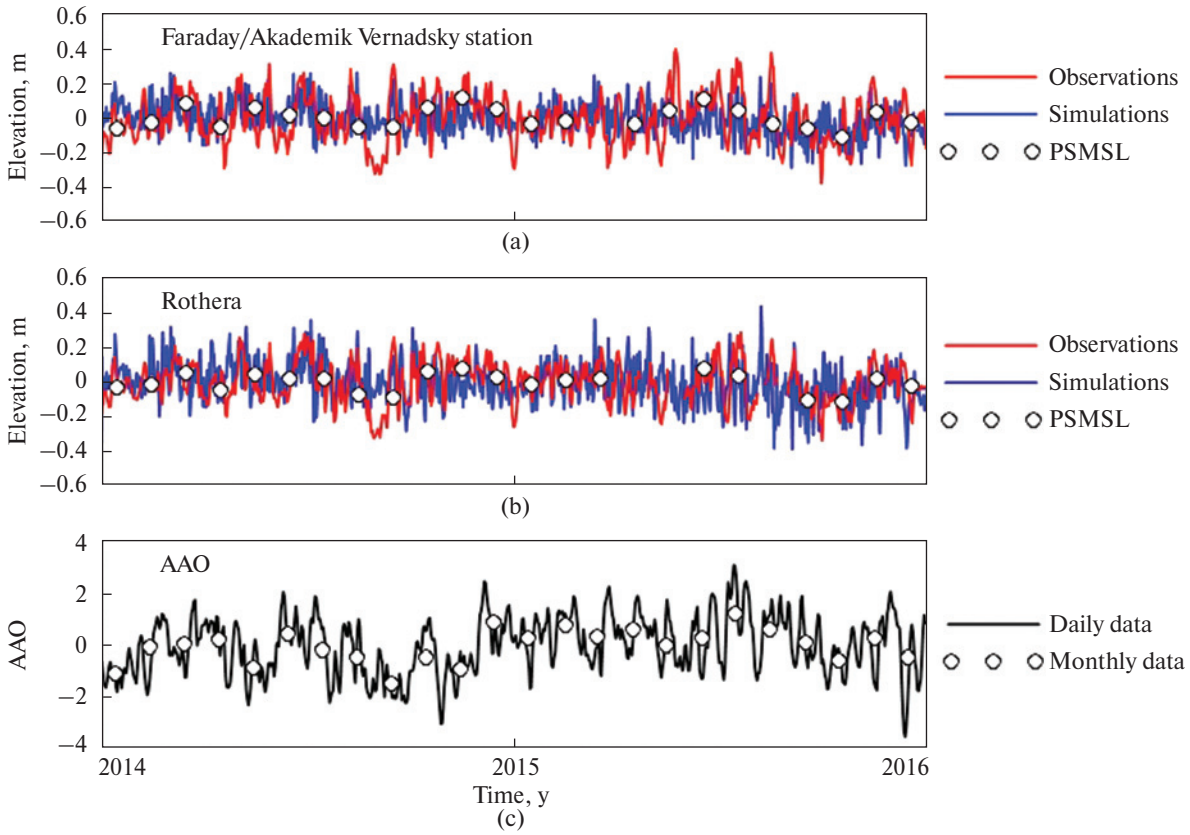

Figure 5. Variations of the daily sea elevations at the Faraday/Akademik Vernadsky (a) and Rothera (b) stations (UHSLC, 2020) with the imposed variations of sea level calculated by model and mean month data PSMSL (2020) and (c) normalized Antarctic Oscillation index (CPC, 2020)

It is important that variations of elevations at stations Faraday/Akademik Vernadsky and Rothera are similar, especially on the scale of months, despite the differences in local bathymetry at the stations. It should be expected that the observed variations of level may be associated with large-scale variations in the wind field. The AAO is the dominant pattern of intraseasonal tropospheric circulation variations. Aoki (2002) found that coherent intraseasonal variations in Antarctic coastal sea levels have significant correlations with the AAO index. The daily and monthly values of AAO index (Gong & Wang, 1999) in Fig. 5c also showed similarity with sea elevations at monthly scale.

The sea level scalegrams *SC* (1) were used to estimate the shift-averaged periods and the amplitudes of the coefficients $W_A(a_i, b_j)$ characterizing dominant periods of sea level oscillations. The scalegrams of observed sea level variations in 2014 and 2015 at stations Faraday/Akademik Vernadsky and Rothera are given in Fig. 6a and b. On the scale of 1–150 days the largest amplitudes of the level scalegrams were observed for a period of approximately 100 days in 2014 and 120 days in 2015 at both stations. A secondary maximum of *SC* was observed for a period of 40 days in 2014, but in 2015 it disappeared. Instead such secondary maximum was observed for a period of about 22–23 days. The largest amplitudes of scalegrams for AAO were observed for a period of 105 days in 2014 and 123 days in 2015. The secondary maximums for periods of 49 and 25 days were presented in AAO scalegrams for 2014, whereas corresponding values of periods for 2015 were 57 and 25 days. The correlation coefficients between sea level scalegrams for stations Faraday/Akademik Vernadsky and Rothera and for

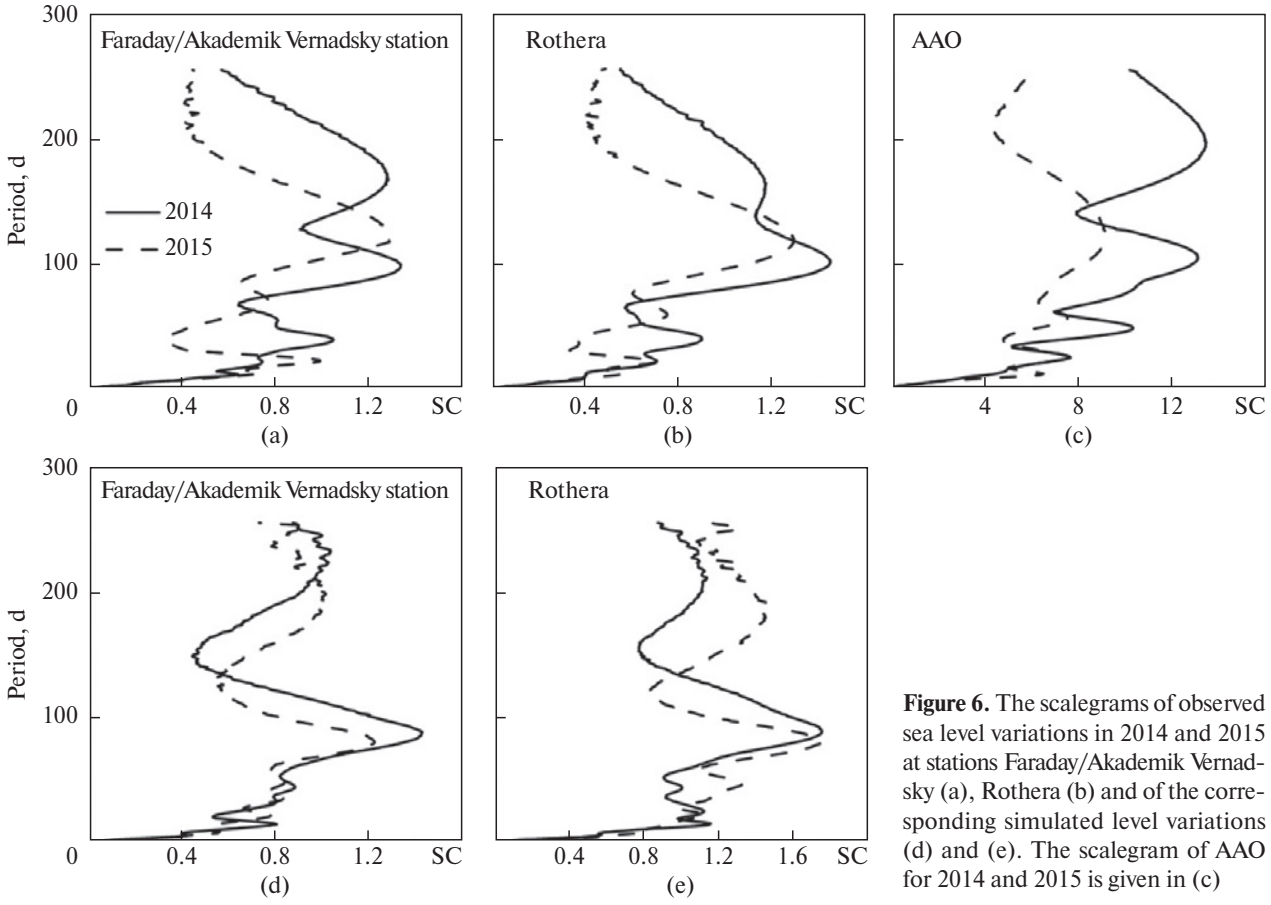

Figure 6. The scalegrams of observed sea level variations in 2014 and 2015 at stations Faraday/Akademik Vernadsky (a), Rothera (b) and of the corresponding simulated level variations (d) and (e). The scalegram of AAO for 2014 and 2015 is given in (c)

AAO scalegrams for 2014 were 0.84 and 0.86, respectively, whereas for 2015 they were 0.87 and 0.90, respectively. This confirms the relationship between intraseasonal processes in the ocean in West Antarctica and AAO at the scale of about 100 days as obtained by Aoki (2002) using spectral analysis.

The scalegrams of simulated sea level variations in 2014 and 2015 at locations of stations Faraday/Akademik Vernadsky and Rothera are given in Fig. 6d and 6e. On the scale of 1–150 days the largest amplitudes of level scalegrams were obtained for a period of approximately 88 days in 2014 and 80 days in 2015 at both stations. A secondary maximum was observed for a period of 14 days in 2014 and 21 days in 2015. The correlation between simulated sea level scalegrams and AAO was lower than for observations: values of correlation coefficients for locations of stations Faraday/Akademik Vernadsky and Rothera were 0.69 and 0.79, whereas for 2015 the relationships were statistically insignificant. These differences with observations can be explained by the difference in forcing by winds from ERA5 reanalysis and boundary conditions on the western boundary of the computational domain.

4 Conclusions

The circulation model SCHISM augmented by the ice model FESIM was used to simulate seasonal and intraseasonal variations of the circulation, sea level and thermohaline structure in the Bellingshausen Sea and on the shelf of the WAP. The results of modelling of the sea level, temperature, and salinity fields in the period 2014–2015 were compared with the available observational data. The simulated horizontal and vertical distribution of subsurface layer with

minimum of potential temperature T_{min} (Winter Water) which is a remnant of mixed layer formed as a result of convection in austral winter were considered. The depth of minimum of potential temperature T_{min} varied in the range of 10–100 m increasing northward. The value of T_{min} also increased to the north from –1.8 to 1.2 °C. The intraseasonal oscillations of sea level computed by the model for 2014–2015 were analysed together with data of observations in the tidal stations Faraday/Akademik Vernadsky and Rothera located at the coast of WAP. In the range of 1–150 days the largest amplitudes of the level scalegrams were observed for a period of approximately 100 days in 2014 and 120 days in 2015 at both stations. The largest amplitudes of modelled level scalegrams were observed with a period of approximately 88 days in 2014 and 80 days in 2015 at both stations. The largest amplitudes of scalegrams for Antarctic Oscillation (AAO) were observed for a period of 105 days in 2014 and 123 days in 2015. The corresponding correlation coefficients related scalegrams for the sea level and AAO for 2014 were 0.84 and 0.86, respectively, whereas for 2015 they were 0.87 and 0.90, respectively. It was concluded that the relationship between intraseasonal processes in the ocean in the West Antarctica and AAO existed at a scale of about 100 days. In the future, it is necessary to study processes of similar periods in other regions of Antarctica and using longer series of calculations.

Author contribution. VM: conceptualization. IB, KT: numerical modeling. IB, KT, AB: data processing. VM, IB, KT, AB: data analysis. VM, IB, KT: writing — original draft. VM, IB: writing — review and editing. All authors have read and agreed to the published version of the manuscript.

Conflict of Interest. The authors declare that they have no conflict of interest.

Acknowledgments: The work was supported by the State Institution National Antarctic Scientific Center Ministry of Education and Science of Ukraine, contract №Н/01-2019 "Modelling of seasonal variability of temperature, salinity, currents and sea ice of the Bellingshausen Sea and on the shelf of the Antarctic Peninsula".

References

Aoki, S. (2002). Coherent sea level response to the Antarctic Oscillation. *Geophysical Research Letters*, 29(20), 11-1–11-4. https://doi.org/10.1029/2002GL015733

Bouillon, S., Fichefet, T., Legat, V., & Madec, G. (2013). The elastic-viscous-plastic method revisited. *Ocean Modelling*, 71, 2–12. http://doi.org/10.1016/j.ocemod.2013.05.013

COPERNICUS (2020). Marine Service. Retrieved August 12, 2020, from http://marine.copernicus.eu/services-portfolio/access-to-products

CPC (Climate Prediction Centre) (2020). Antarctic Oscillation. Retrieved October 10, 2020, from https://www.cpc.ncep.noaa.gov/products/precip/CWlink/daily_ao_index/aao/aao.shtml

Danilov, S., Wang, Q., Timmermann, R., Iakovlev, N., Sidorenko, D., Kimmritz, M., Jung, T., & Schröter, J. (2015). Finite-Element Sea Ice Model (FESIM), version 2. *Geoscientific Model Development*, 8, 1747–1761. https://doi.org/10.5194/gmd-8-1747-2015

Dinniman, M. S., Klinck, J. M., & Smith, W. O. Jr. (2011). A model study of Circumpolar Deep Water on the West Antarctic Peninsula and Ross Sea continental shelves. *Deep Sea Research Part II: Topical Studies in Oceanography*, 58(13–16), 1508–1523. https://doi.org/10.1016/j.dsr2.2010.11.013

ERA5 (2020). Retrieved August 12, 2020, from https://www.ecmwf.int/en/forecasts/datasets/reanalysis-datasets/era5

GEBCO (General Bathymetric Chart of the Oceans) (2020). Retrieved August 12, 2020, from https://www.gebco.net/data_and_products/gridded_bathymetry_data

Gong, D. & Wang, S. (1999). Definition of Antarctic Oscillation index. *Geophysical Research Letters*, 26(4), 459–462. https://doi.org/10.1029/1999GL900003

Gordon, A. L. (1971). Antarctic polar front zone. In J. L. Reid (Ed), *Antarctic Research Series. Antarctic Oceanology I* (15, pp. 205–222).

Graham, J. A., Dinniman, M. S., & Klinck, J. M. (2016). Impact of model resolution for on-shelf heat transport along the West Antarctic Peninsula. *Journal of Geophysical Research: Oceans*, 121(10), 7880–7897. https://doi.org/10.1002/2016JC011875

Holland, P. R., Jenkins, A., & Holland, D. M. (2010). Ice and ocean processes in the Bellingshausen Sea, Antarctica. *Journal of Geophysical Research: Oceans*, 115(C5). https://doi.org/10.1029/ 2008JC005219

Hunke, E. C. & Dukowicz, J. K. (1997). An Elastic-Viscous-Plastic model for sea ice dynamics. *Journal of Physical Oceanography*, 27(9), 1849–1867. https://doi.org/10.1175/1520-0485(1997)027<1849:AEVPMF>2.0.CO;2

Klinck, J. M., Hofmann, E. E., Beardsley, R. C., Salihoglu, B., & Howard, S. (2004). Water-mass properties and circulation on the west Antarctic Peninsula Continental Shelf in Austral Fall and Winter 2001. *Deep Sea Research Part II: Topical Studies in Oceanography,* 51(17–19), 1925–1946. https://doi.org/10.1016/j.dsr2.2004.08.001

Maderich, V., Terletska, K., Brovchenko, I., & Bezhenar, A. (2018). Modeling summer circulation and distribution of temperature and salinity in the Bellingshausen Sea and on the Antarctic Peninsula shelf. *Ukrainian Antarctic Journal,* 1(17), 48–57. https://doi.org/10.33275/1727-7485.1(17).2018.31

Maderich, V., Terletska, K., Brovchenko, I., & Pishniak, D. (2019). Long-term variations of the sea level on the western coast of the Antarctic Peninsula. *Ukrainian Antarctic Journal*, 1(18), 93–102. https://doi.org/10.33275/1727-7485.1(18).2019.134

Martinson, D. G., Stammerjohn, S. E., Iannuzzi, R. A., Smith, R. C., & Vernet, M. (2008). Western Antarctic Peninsula physical oceanography and spatio-temporal variability. *Deep Sea Research Part II: Topical Studies in Oceanography*, 55(18–19), 1964–1987. https://doi.org/10.1016/j.dsr2.2008.04.038

MATLAB (2020). https://se.mathworks.com/help/wavelet/time-frequency-analysis.html

Moffat, C. & Meredith, M. (2018). Shelf-ocean exchange and hydrography west of the Antarctic Peninsula: a review. *Philosophical Transactions of the Royal Society A*, 376(2122), Article 20170164. https://doi.org/10.1098/rsta.2017.0164

Neverovsky, I. P., Popov, Y. I., Sytov, V. N., & Matygin, A. S. (2015). The first observation of the cold intermediate layer on shelf Antarctic peninsula. *Ukrainian Antarctic Journal*, 14, 114–123. https://doi.org/10.33275/1727-7485.14.2015.179

PSMSL (Permanent Service for Mean Sea Level) (2020). Tide Gauge Data. Retrieved September 12, 2020, from http://www.psmsl.org/data/obtaining

Regan, H. C., Holland, P. R., Meredith, M. P., & Pike, J. (2018). Sources, variability and fate of freshwater in the Bellingshausen Sea, Antarctica. *Deep Sea Research Part I: Oceanographic Research Papers,* 133, 59–71. https://doi.org/10.1016/j.dsr.2018.01.005

Scargle, J. D. (1997). Wavelet and other multi-resolution methods for time series analysis. In G. J., Babu, & E. D. Feigelson (Eds), *Statistical Challenges in Modern Astronomy II* (pp. 333–347). Springer.

Smith, D. A., Hofmann, E. E., Klinck, J. M., & Lascara, C. M. (1999). Hydrography and circulation of the west Antarctic Peninsula continental shelf. *Deep-Sea Research, Part I: Oceanographic Research Papers,* 46, 925–949.

Torrence, C. & Compo, G. P. (1998). A practical guide to wavelet analysis. *Bulletin of the American Meteorological Society*, 79, 61–78. https://doi.org/10.1175/1520-0477(1998)079<0061:APGTWA>2.0.CO;2

UHSLC (University of Hawaii Sea Level Center) (2020). Tide gauge data. Retrieved October 10, 2020, from http://uhslc.soest.hawaii.edu/data

Zeng, X., Zhao, M., & Dickinson, R. E. (1998). Intercomparison of bulk aerodynamic algorithms for the computation of sea surface fluxes using TOGA COARE and TAO data. *Journal of Climate*, 11(10), 2628–2644. https://doi.org/10.1175/1520-0442(1998)011<2628:IOBAAF>2.0.CO;2

Zhang, Y. J., Ateljevich, E., Yu, H.-C., Wu, C. H., Yu, J. C. S. (2015). A new vertical coordinate system for a 3D unstructured-grid model. *Ocean Modelling*, 85, 16–31. https://doi.org/10.1016/j.ocemod.2014.10.003

Zhang, Y. J., Ye, F., Stanev, E. V., & Grashorn, S. (2016). Seamless cross-scale modelling with SCHISM. *Ocean Modelling*, 102, 64–81. https://doi.org/10.1016/j.ocemod.2016. 05.002

Received: 23 October 2020
Accepted: 24 December 2020

І. Бровченко, В. Мадерич*, К. Терлецька, А. Беженар

Інститут проблем математичних машин і систем НАН України, м. Київ, 03187, Україна

***Автор для кореспонденції**: vladmad@gmail.com

Моделювання сезонних та внутрішньо-сезонних варіацій циркуляції, температури, солоності і рівня моря Беллінсгаузена та на шельфі Антарктичного півострова

Реферат. Метою дослідження є моделювання сезонних та внутрішньо-сезонних коливань циркуляції, рівня моря, температури та солоності в морі Беллінсгаузена та на шельфі західної частини Антарктичного півострова (ЗАП). Для моделювання застосовуються чисельні методи з використанням моделі Semi-implicit Cross-scale Hydroscience Integrated System Model неструктурованою трикутною горизонтальною сіткою та вертикальною локальною сигма-системою координат та динамічно-термодинамічною моделлю льоду Finite-Element Sea Ice Model. Потоки тепла, імпульсу та солі задавалися на поверхні океану згідно з реаналізом ERA5. На відкритих границях вертикальний розподіл температури та солоності визначався за реаналізом COPERNICUS. На відкритій західній границі обчислювальної області також був заданий вертикальний розподіл швидкості течій згідно COPERNICUS. На відкритій східній границі були задані відхилення рівня згідно COPERNICUS. Аналіз часових варіацій рівня проводився за допомогою вейвлет-аналізу. **Результати** моделювання полів рівня моря, температури та солоності в період 2014—2015 рр. були порівняні з наявними даними спостережень на шельфі ЗАП, включаючи дані Української антарктичної експедиції. Наведено розраховані горизонтальний та вертикальний розподіли проміжного шару з мінімумом потенційної температури T_{min} (Зимова Вода). Глибина мінімуму T_{min} коливається в діапазоні 10—100 м, збільшуючись на північ. Значення T_{min} також збільшуються на північ від −1.8 до 1.2 °С. Проаналізовані внутрішньо-сезонні коливання рівня моря, розраховані за моделлю на 2014—2015 роки, разом із даними спостережень на припливних станціях «Фарадей/Вернадський» та «Розера», розташованих на узбережжі ЗАП. У діапазоні 1—150 днів найвищі амплітуди скейлеграм рівня спостерігались з періодом приблизно 100 днів у 2014 році та 120 днів у 2015 році на обох станціях. Найвищі амплітуди модельних скейлеграм рівня спостерігались з періодом приблизно 88 днів у 2014 році та 80 днів у 2015 році на обох станціях. Найбільші амплітуди скейлеграм для Антарктичного Коливання (АК) спостерігались з періодом 105 днів у 2014 році та 123 днів у 2015 році. Відповідні коефіцієнти кореляції між спостережуваними скейлеграмами рівня на станціях та АК за 2014 рік становили 0.84 та 0.86, відповідно, тоді як для 2015 року вони були 0.87 та 0.90, відповідно. Зроблено **висновок** про взаємозв'язок внутрішньо-сезонних процесів в океані в Західній Антарктиді та АК на часовому масштабі близько 100 днів.

Ключові слова: Антарктичний півострів, антарктична станція Фарадей/«Академік Вернадський», Зимова Вода, внутрішньо-сезонні коливання, модель SCHISM, море Беллінсгаузена